UNITED STATES ATOMIC ENERGY COMMISSION

NORTHERN STATES POWER COMPANY

Monticello Nuclear Generating Plant Docket No. 50-263

REQUEST FOR AUTHORIZATION OF
MODIFICATIONS TO GASEOUS RADWASTE SYSTEM

PROVISIONAL OPERATING LICENSE NO. DPR-22

Supplemental Information to
Change Request No. 2

Northern States Power Company, a Minnesota corporation, proposed certain modifications to the gaseous radwaste system by submission of Change Request No. 2 dated April 1, 1971. This supplemental information is for clarification on the following items:

(1) Design basis for the filter and computation of shock wave attenuation in the recombiner system.

(2) Verification that the dilution flow to the off-gas stack will be maintained constant.

This supplement contains no restricted or other defense information.

NORTHERN STATES POWER COMPANY

By A V Dienhart
A V Dienhart
Vice President - Engineering

Subscribed and sworn to before me

this 10 day of December, 1971.

John J. Smith
John J Smith
Notary Public, Hennepin County, Minnesota

My Commission Expires March 3, 1976

Notarial Seal

John J. Smith
Notary Public, Hennepin County, Minnesota
My Commission Expires March 3, 1976

RECEIVED
DEC 1 1971

9105010219 711210
PDR ADOCK 05000263
P PDR

5381

NSP

MONTICELLO NUCLEAR GENERATING PLANT

MONTICELLO, MINNESOTA

Regulatory File Cy.

Received w/Ltr Dated 12-10-71

UNIT 1

(USAEC Docket 50-263)

SUPPLEMENTAL ANSWERS TO DRL QUESTIONS

December 1971

NORTHERN STATES POWER COMPANY

MINNEAPOLIS, MINNESOTA

5361

NSP

MONTICELLO NUCLEAR GENERATING PLANT

MONTICELLO, MINNESOTA

UNIT 1

(USAEC Docket 50-263)

SUPPLEMENTAL ANSWERS TO DRL QUESTIONS

December 1971

NORTHERN STATES POWER COMPANY

MINNEAPOLIS, MINNESOTA

ANSWERS TO DRL QUESTIONS

Question #1 - What steps will be taken to insure that the dilution flow to the off-gas stack and the isokinetic probe will be maintained at a constant flow of about 4000 cfm.

Answer - The existing fully redundant stack fans and control systems are currently designed and operated so that the dilution flow to the stack and isokinetic probe is automatically maintained at a constant flow of about 4000 cfm, independent of the fan inlet or stack exhaust conditions. This is accomplished by continuously monitoring stack flow with redundant pitot tubes and using the flow signal feed back to position the stack fan inlet vanes which control the actual flow.

In the proposed system, stack flow will be maintained in exactly the same way, since the only change is the source of dilution air to the stack fans.

Under normal operating conditions, the 4000 cfm dilution flow will be made up of 2000 cfm from the air ejector room ventilation system and 2000 cfm from the proposed storage building ventilation system. Should the flow split between the air ejector room and the storage building become unbalanced, a control damper in the storage building ventilation system can be adjusted from the control room to return the system balance to normal.

In the event the 4000 cfm Standby Gas Treatment System is automatically initiated, the storage building ventilation system (as well as the air ejector room ventilation flow) will be shut down and possible back flow to the storage building stopped by a check damper.

When the Standby Gas Treatment System is being used for containment purge with flows of about 3500 cfm, the ventilation flow from the storage building will be reduced to about 500 cfm. The split of dilution flow to the stack fans will be adjusted as necessary by repositioning the control damper in the storage building ventilation system.

Question #2 - The NSP answer to DRL Question #2 of June 3, 1971, stated in part:

> "Calculations indicate that the overpressure associated with any shock wave propogating from the recombiner system would be attenuated to about 1/10 of its initial value by the effects of expansion and subsequent propogation through the various piping systems to the air compressor inlet filter. To fully insure that no potential shock wave could reach the air compressors, the charcoal filter element has been designed to withstand the full 350 psig over-pressure without failure, and thus the filter element will reflect and/or absorb any potential shock wave to insulate the air compressor from the recombiner system."

Provide the calculational method utilized for computing the shock attenuation and the design basis for the filter. Also, a detonation occurring in the inlet end of the 30 minute delay pipe should be considered.

Answer - As shown in the attached calculation sheets that consider the shock wave resulting from a detonation in the inlet end of the 30 minute decay pipe, the calculational model has been based on conventional shock

tube and shock wave theory as presented by Greene and Toennies (1) and Dryden and von Karman (2). The model has several features that insure conservative results:

(1) The calculations of shock wave attenuation in the various off-gas pipes are based on data developed in either steel or glass shock tubes. The internal surfaces of the off-gas pipes would not be as smooth as the experimental apparatus, and rough surfaces result in increased attenuation.

In addition, elbows or other direction changes in piping systems would tend to reflect a significant fraction of the energy of an incident shock wave and thus result in significant attenuation of the on-going shock wave. However, the calculational model treats elbows as equivalent pipe in accordance with sub-sonic pressure drop theory and, as a result, underestimates the attentuation in the piping system.

(2) The calculational model handles the problem of predicting the shock wave generated in the 6 inch diameter branch line off the 42 inch diameter, 30 minute delay pipe in accordance with conventional shock tube theory. In such a conventional shock tube, a gas reservoir is pressurized, and the high pressure gas is suddenly admitted to the low pressure portion of the shock tube through a quick opening diaphragm. The calculational model assumes that the high pressure short duration (< 0.5 millisecond) shock wave reflected from the discharge end of the 30 minute delay pipe acts the same as the high

pressure gas reservoir. Thus the model equates a static, high pressure reservoir with a very short duration pressure front and consequently overestimates the shock wave in the 6 inch diameter branch pipe.

Based on the calculational model, the shock wave resulting from a hydrogen-oxygen detonation in the inlet end of the 30 minute delay pipe is attenuated to ~ 30 psig by the effects of system attenuation and the subsequent expansion into the off-gas compressor inlet filters. Since the charcoal filter retention elements are being designed to withstand 350 psig overpressure, the charcoal filter element would further attenuate the shock wave, although such additional attenuation is not included in the calculational model.

The ~ 30 psig pressure wave that could possibly propogate into the off-gas compressor suction is smaller than the margin between storage system design pressure and the normal operating pressure; accordingly a pressure wave of this magnitude is not of concern in evaluating the structural integrity of the storage tanks and associated system.

References

(1) Greene, Edward F. and Toennies, J. Peter: "Chemical Reactions in Shock Waves"; Academic Press, Inc. 1964

(2) Dryden, H. L. and von Karman, Th. "Advances in Applied Mechanics" Volume VI; Academic Press, Inc. 1960

CLIENT NSP TASK NO. Pay A DATE 11/26 PAGE 1 OF 13

SUBJECT Shock in bio pipe BY PDA/PWF

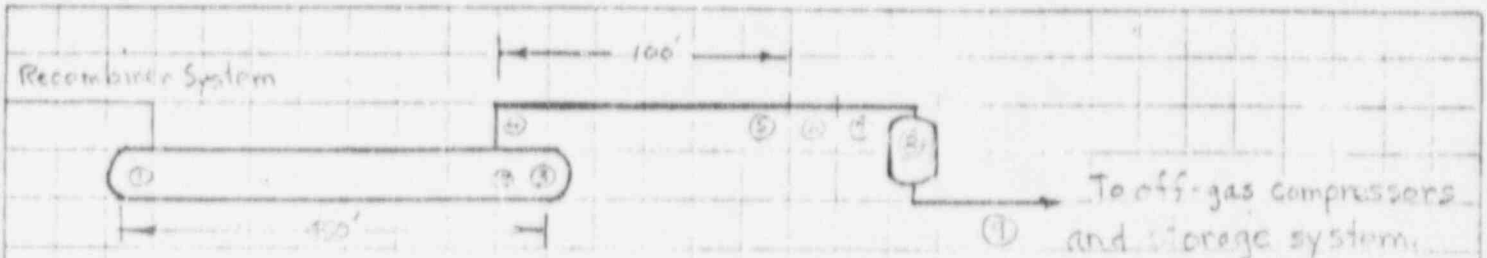

Summary of Results

	M_s	P
① Detonation in recombiner system end of 42" ID delay pipe	5.3	650 psia
② Incident shock wave at end of 42" ID delay pipe.	3.7	390 psia
③ Reflected shock wave at end of 42" ID delay pipe.	—	1700 psia
④ Incident shock wave into 4" ID off-gas pipe.	3.8	340 psia
⑤ Shock wave at end of 6" ID off-gas pipe.	2.66	165 psia
⑥ Shock wave after contraction from 6" to 3"	3.0	240 psia
⑦ Shock wave after contraction from 3" to 2" pipe	3.5	300 psia
⑧ Shock wave after expansion from 3" pipe into 24" ID filter body.	1.2	31.5 psia
⑨ Shock wave after reflection	1.44	47 psia

① From the recombiner system design basis, the detonation shock wave from a stoichmetric mixture of H_2-O_2 at 20psia is: Peak Pressure = 650psia ← ①
Mach No = 5.3

① → ⑦ Attenuation from Pipe Wall

Treat attenuation as a deviation from ideal behavior in a standard shock tube as discussed by Greene & Toennies in Attachment #1.

From Table 5.5, attenuation of shock speed $\frac{\Delta u}{u}$ per meter of travel is seen to vary from 0 to a high of ~0.1. For the large (61cm) diameter, stainless steel tube, $\frac{\Delta u}{u}$ varied from 0 to 0.007 for shocks of M = 11-24. Because the carbon steel delay pipe (47" ID) would be expected to be rougher on the inside walls than a stainless steel shock tube, an allowance factor for $\frac{\Delta u}{u}$ per meter of 0.025 is considered conservative.

CLIENT NSP TASK NO. P&A DATE 11/26 PAGE 3 OF 13

SUBJECT Shock in big pipe BY PDA/RWP

Also, assume that only 100 m (ie ~300 ft) of the 450 ft pipe is available for attenuation.

Then $\Delta u = u \left(\frac{\Delta u}{u \Delta x}\right) \Delta x$; $\frac{\Delta u}{u} = -0.0035 \Delta x$

Integrating: $\ln u = -0.0035 x + c$

$u = 5.3 e^{-0.0035 x}$; $x = 100$

$u = 5.3 e^{-0.35} = (5.3 \times 0.705) = 3.7$ M

Pressure from Figure = 340 psia

Check on $\bar{A}$

From Attachment #1 $\frac{P_2}{P_1} - 1 = \left(\frac{P_2}{P_1} - 1\right)_{ideal} e^{-\frac{\bar{A} x}{D}}$

$\frac{P_2}{P_1} - 1 = \frac{340}{20} - 1 = 16$

$\left(\frac{P_2}{P_1} - 1\right)_{ideal} = \frac{680}{20} - 1 = 31.5$

$e^{-\frac{\bar{A} x}{D}} = \frac{16}{31.5} = 0.51$

$x = 100$ m $\doteq$ 330 ft

$D = 12"$ = 1 ft

$$0.51 = e^{-\frac{\bar{A}(240)}{0.3}} \; e^{-95\bar{A}}$$

Taking log(n) of both sides

$$\log_n 0.51 = -95\bar{A}$$

$$-0.68 = -95\bar{A}$$

$$\bar{A} = \frac{-0.68}{-95} = 7.2 \times 10^{-3}$$

Attachment #1 states $\bar{A}$ vary $0.6 \rightarrow 6 \times 10^{-3}$ for weak shocks; 7.2×10^{-3} appears to be in right size range for shock of Mach 5.3.

② → ③ Looking at reflected shock at end of 47" delay pipe, for Mach 3.7 reflected shock is (2.3)(55) = 1700 psia from Figure 2. ←

③ → ② To compute the shock wave into the branch line, consider the gas in the end of the 47" delay pipe to be a driver gas for a shock tube (t2) at a pressure of 1700 psia.

Solving the driver gas, shock tube equation

$$\frac{P_4}{P_1} = \left[\frac{2\gamma_1 M_s^2 - (\gamma_1 - 1)}{\gamma_1 + 1}\right]\left[1 - \frac{(\gamma_4 - 1)}{(\gamma_1 + 1)}\frac{a_1}{a_4}\left(M_s - \frac{1}{M_s}\right)\right]^{-\left(\frac{2\gamma_4}{\gamma_4 - 1}\right)}$$

where $\frac{P_4}{P_1}$ = driver gas pressure ratio $\frac{1700}{20} = 85$

γ_1 = specific heat ratio $\frac{C_p}{C_v}$ @ $T_1 = 300°K = 1.4$

γ_4 = specific heat ratio $\frac{C_p}{C_v}$ @ $T_4 = 2000°K = 1.3$

$\frac{a_1}{a_4}$ = speed of sound ratio between air at T_1 and air at T_4

$$\frac{a_1}{a_4} = \sqrt{\frac{T_1}{T_4} \cdot \frac{\gamma_1}{\gamma_4}} = \sqrt{\frac{300}{2000} \cdot \frac{1.4}{1.3}} = 0.4$$

Solving for Ms by trial and error yields:

$M_s = 3.8$

P_2 = [illegible] psia from Figure 1

As a check, the result was compared with experimental data reported in Figures 5.8, 5.9 and 5.10 of Attachment #1. For the above case; ie $\frac{P_4}{P_1}$ = [illegible], $\log_{10}\frac{P_4}{P_1} = 1.9$; measured Mach Numbers for [illegible] to air $\left(\frac{a_1}{a_4} = 0.25\right)$ which would give weaker shocks are in range 3.5 [illegible] OK

④ → ⑤ From data for ~6" tubes and $M_s \hat{=} 3.4$ from Table 5.5 of Attachment # 1, assume

$\frac{\Delta u}{u_1}$ /meter = 0.005.

The piping system from 4 → 5 has 1.5 90° elbows which would be expected to significantly attenuate the shock wave. For this calculation, treat the elbows as equivalent pipe for sub-sonic gas flow*; Le = (40)(½)(5) = 100 ft.

Total length = 200 ft = $\frac{200}{(3.28)}$ = 60 meters

from above: $u = u_1 e^{-(.005)(60)} = 3.8 \times e^{-.3}$

$u = (3.8)(0.7) = 2.66$

$u = M_s = 2.66$ ⑤

$P_5 = 165$ psia (from Figure 1)

* Perry's Chemical Eng. Handbook p 5-33; Le = 40

CLIENT NSC TASK NO. Part A DATE 11/26 PAGE 7 OF 13

SUBJECT Shock tube design BY PDA/PWE

Check on $\bar{A}$

$$\left(\frac{165}{20} - 1\right) = \left(\frac{340}{20} - 1\right) e^{-\frac{\bar{A} \cdot x}{D}}$$

$$7.25 = 16\, e^{-\frac{\bar{A} x}{D}}$$

$$0.45 = e^{-\frac{\bar{A} \times 200}{12}}$$

Taking logs: $-0.8 = \bar{A} \times 400$

$$\bar{A} = \frac{0.8}{400} = 2 \times 10^{-3}$$

From Mach curve #1, $\bar{A} = 0.6 \to 6 \times 10^{-3}$ OK

⑤ ⑥ For calculation of contraction from 6" to 2" pipe Figure #4 of Attachment #2 is utilized. Note Figure 4 is based on a $\gamma = 1.66$ rather than the $\gamma = 1.40$ for air. Data presented in Table 7 of Attachment #2 indicates that results based on $\gamma = 1.66$ will be conservative for $\gamma = 1.4$.

$P_1 = 20$ psia

$P_2 = 165$ psia

$M_s = 2.66$

Contraction ratio $= \frac{6^2}{2^2} = 9:1$

CLIENT NSP TASK NO. Rev A DATE 11/26 PAGE 8 OF 17

SUBJECT Shock in big pipe BY PDA / [illegible]

Using data from Figure 1 of Attachment #2 for contraction ratio of 5:1 and $M_s = 2.66$;

$$\frac{P_3 - P_1}{P_2 - P_1} = 1.5$$

$$P_3 - 20 = (1.5)(165 - 20)$$

$$P_3 = 240 \text{ psia}$$

⑥

$$\frac{P_3}{P_1} = \frac{240}{20} = 12 \; ; \; M_s = 3$$

⑥ → ① For contraction of 3" to 2", use same method as calculation of ⑤ → ⑥ above, using $M_s = 3.0$ and contraction ratio 2:1 data from Figure 4 of Attachment #2.

$$\frac{P_2 - P}{P_2 - P_1} = \frac{P_2 - 20}{220} = 1.2 \qquad P_1 = 20$$

$$P_2 = 220 + 20 = 300 \text{ psia} \qquad P_3 = 240 \text{ psia}$$

$$\frac{P_3}{P_1} = \frac{300}{20} = 15$$

①

From Figure 1, $M_s = 3.5$

CLIENT NSP TASK NO. Rev A DATE 11/26 PAGE 9 OF 13

SUBJECT Shore in big pipes BY PHA/[illegible]

(7) → (8) For expansion, of a 2" pipe into a 24" ID filter body, utilize data from Figure 7 of Attachment # 2.

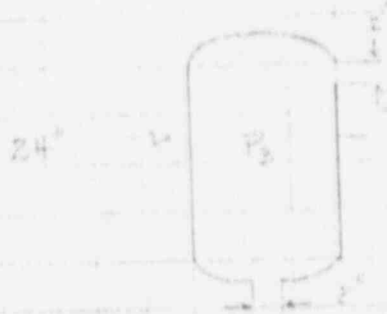

$M_s = 3.5$

$P_5 = 200$ psia

Expansion ratio $= \frac{24^2}{2^2} = 144 \hat{=} \infty$

$P_1 = 20$ psia

For $M_s = 3.5$, From Figure 7

$$\frac{A_1}{A_2}\frac{(P_2 - P_1)}{(P_5 - P_1)} = 6.0$$

$$(P_2 - P_1) = \frac{300 - \ }{144}(6.0)$$

$$P_2 - P_1 = \frac{280(6)}{144} = 11.5$$

$P_2 = 31.5$ psia

$$\frac{P_2}{P_1} = \frac{31.5}{20} = 1.57$$

CLIENT NSP TASK NO. Rev A DATE 11/26 PAGE 10 OF 13

SUBJECT Shock in big pipe BY M.A/EME

From equation for Figure 1

$$\frac{P_2}{P_1} = \frac{2M_s^2\gamma_1 - (\gamma_1 - 1)}{\gamma_1 + 1}$$

$$\frac{P_2}{P_1} = 1.57$$

$$\gamma_1 = 1.4$$

$$1.57 = \frac{2M_s^2(1.4) - 0.4}{2.4}$$

$$M_s^2 = \frac{(2.4)(1.57) + 0.4}{2.8} = \frac{3.7 + 0.4}{2.8} = \frac{4.1}{2.8} \quad 1.46$$

$$M_s = \sqrt{1.46} = 1.2 \quad (3)$$

$P_2 = 31.5$ psia

(2) (3) For the conservation out of the 24" filter with a 2 pipe Figure 5 of Attachment "2. Note Figure 5 is drawn for $\gamma = 1.67$ which yields a conservative result for $\gamma = 1.40$.

From Figure 5, $P_2 = 31.5$

$M_s = 1.2$

$$\frac{P_3}{P_2} = 1.5$$

$P_3 = (1.5)(31.5) = 47.2$ psia

$$\frac{P_2}{P_1} = \frac{47}{20} = 2.3$$

To calculate M_2

$$M_2^2 = \frac{(2.4)(2.3) + 0.4}{2.8} = \frac{5.5 + 0.4}{2.8} = \frac{5.9}{2.8} = 2.1$$

$$M_2 = \sqrt{2.1} = 1.44$$

(11)

$P = 47$ psia ≈ 30 psig

CLIENT NSP TASK NO. Rev A DATE 11/26 PAGE 12 OF 13

SUBJECT Shock in big pipe BY PVA/EWS

Figure 1

Shock Wave Pressure Ratio P_2/P_1 vs. Mach No (in air)

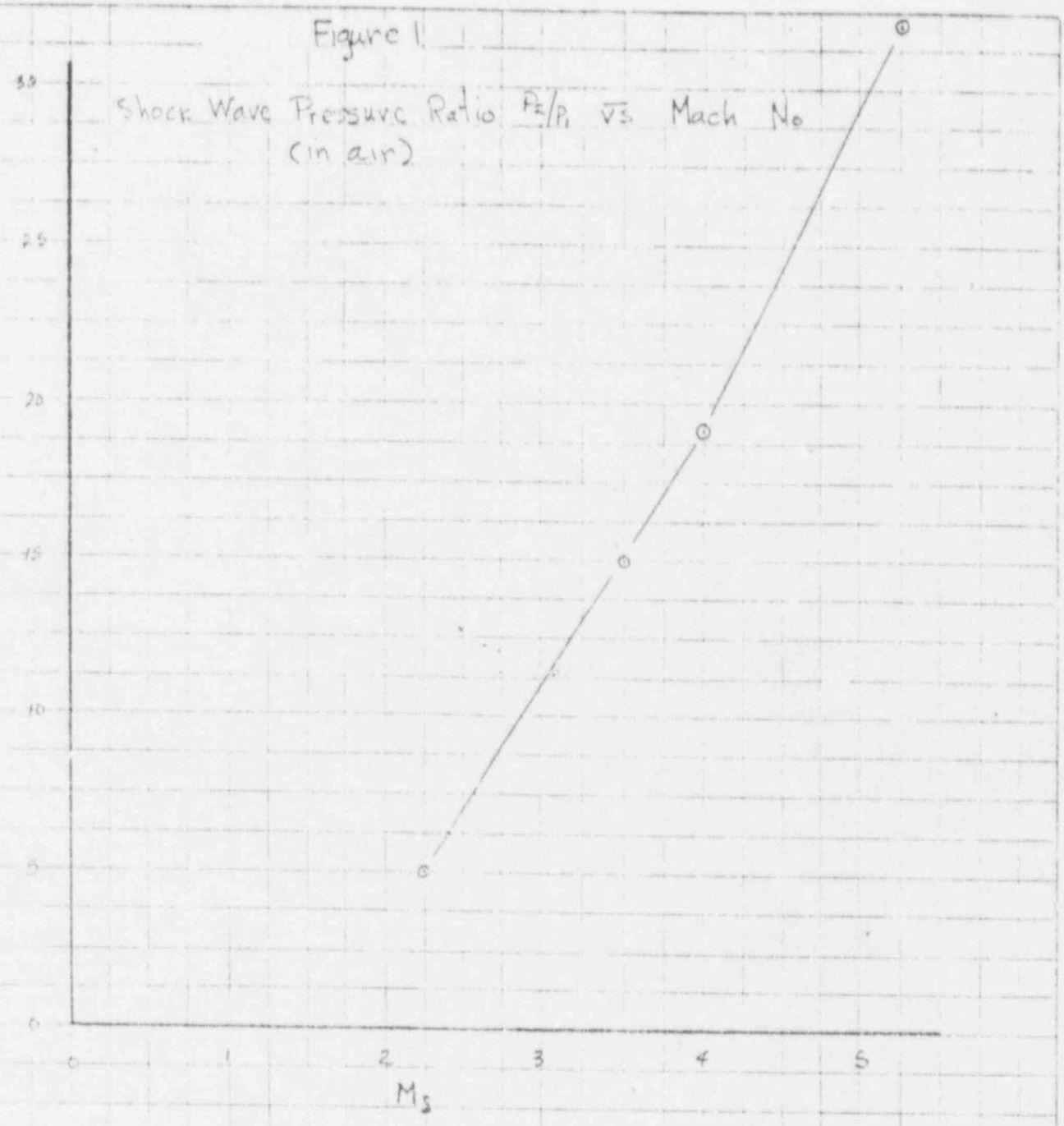

Curve based on shock front equations; γ_1 = specific heat ratio $\frac{C_p}{C_v} = 1.4$

$$\frac{P_2}{P_1} = \frac{2M_s^2\gamma_1 - (\gamma_1 - 1)}{(\gamma_1 + 1)} \quad \text{---}$$

Figure 2

Reflected Shock Wave Pressure Ratio vs. Mach No (in air)

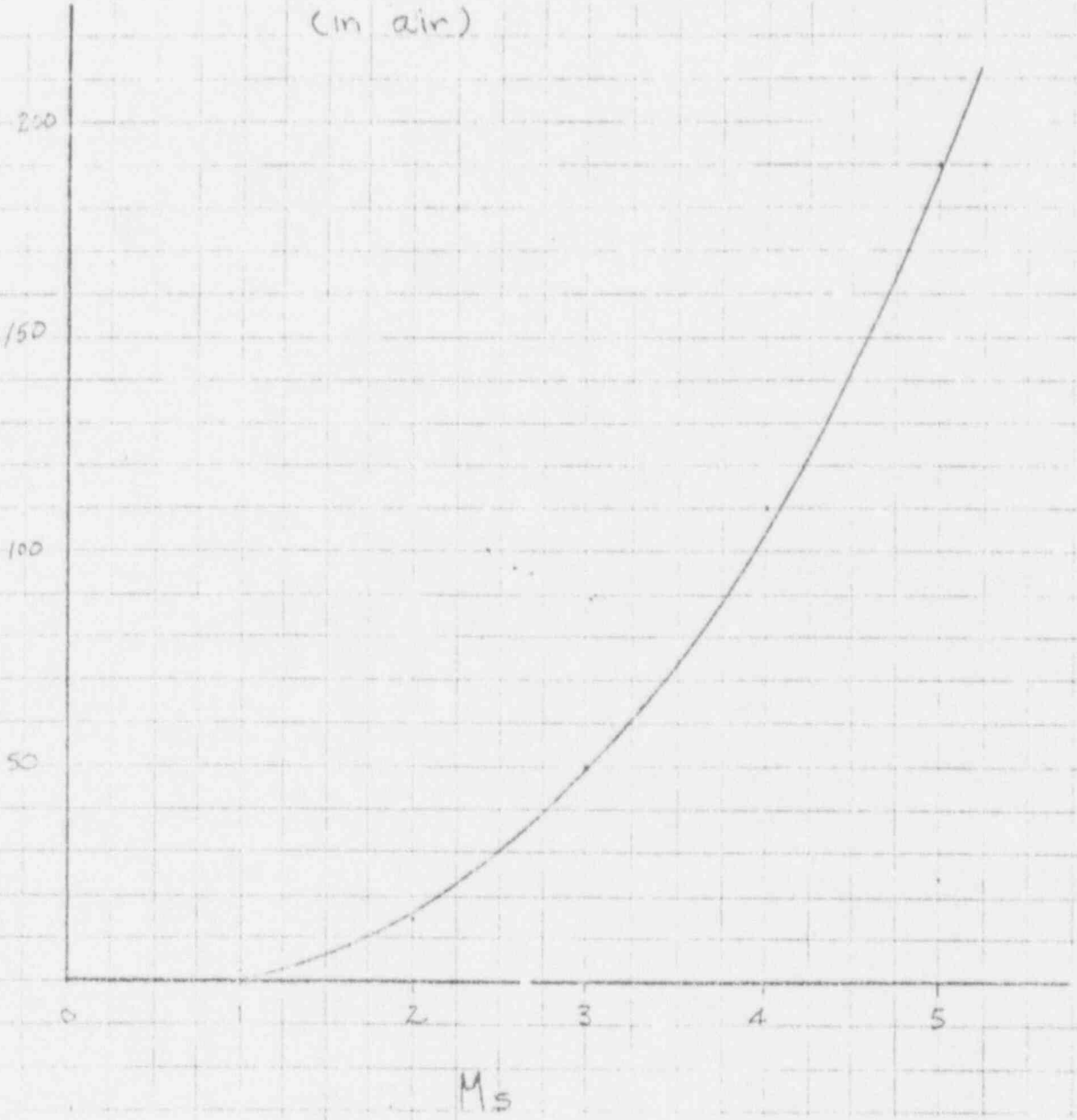

Curve based on reflected shock equation; $\gamma_1 = 1.4$ for air

$$\frac{P_S}{P_1} = \left[\frac{2\gamma_1 M_S^2 - (\gamma_1 - 1)}{\gamma_1 + 1}\right]\left[\frac{(3\gamma_1 - 1)M_S^2 - 2(\gamma_1 - 1)}{(\gamma_1 + 1)^2 M_S^2}\right]$$

ATTACHMENT # 1

Chemical Reactions in Shock Waves

by
EDWARD F. GREENE
Department of Chemistry,
Brown University
and
J. PETER TOENNIES
Physikalisches Institut der
Universität, Bonn

1964
ACADEMIC PRESS INC.
NEW YORK, NEW YORK

be proposed for the pressure waves which result from the mixing of the driver and low pressure gases. The maximum shock strength occurred at increasing distances from the diaphragm as the shock strength increased, and some shocks were still accelerating at the end of his 13 m tube (8·9 cm square cross section). He measured opening times of about 600 μsec[1] for scored stainless steel diaphragms 0·25–0·9 mm thick.

2. Deviations arising from interactions with the shock tube walls

For most applications of shock waves the presence of a formation decrement and the significant time required for the formation of shocks after the bursting of the diaphragm would not in themselves be serious deviations from ideal behaviour because a measurement of the shock velocity, once the shock became planar, would still determine the shock properties completely. Much more important are deviations from the idealized shock tube flow which arise because of energy and momentum losses to the shock tube walls. These losses greatly complicate the analysis of the flow because the boundary layer on the walls spoils the one dimensional flow by introducing a radial component, and the attenuation means that the shock compression is not perfectly steady but becomes somewhat time dependent.

Because shock velocities are the most easily measured shock property, the determination of the deceleration of the shock as it moves along a tube is the most common approach to a study of the deviations from ideal flow. Many experimenters have shown that the attenuation at successive intervals down a shock tube may be substantial, sometimes as great as 1 percent per meter of travel. Table 5.5 gives more detailed results for a number of particular cases.

These tubes all had glass or metal surfaces of normal smoothness and there seems to be no large difference between metal and glass. However, when the surface of the shock tube is artificially roughened, for instance by covering it with sand paper, the attenuation is markedly increased.[2]

For gases with large heat capacities (e.g. acetylene or a mixture in chemical equilibrium) the attenuation seems to be considerably reduced.

Emrich and Wheeler[3] have tabulated the results of a number of studies, particularly of weak shocks, in terms of a simple exponential formula

$$\frac{p_2}{p_1} - 1 = \left(\frac{p_2}{p_1} - 1\right)_{(x=0)} e^{-\lambda x/D} \qquad \ldots 5.6$$

1. See Hooker, W. J., *Phys. Fluids*, **4**, 1451 (1961) and Glass, I. C. and Rose, P. H. *ibid.* **6**, 668 (1963) for additional but similar results on diaphragm opening times.
2. Duff, R. E., *J. Appl. Phys.*, **23**, 1232 (1952).
3. Emrich, R. J. and Wheeler, D. B. Jr., *Phys. Fluids*, **1**, 14 (1958).

TABLE 5.5

Attenuation of Shocks in Tubes

Shock Tube		Driver Gas	Heated Gas	p_1 mm	M_s	$\Delta u_s/u_s$ per meter	Distance from Diaphragm m	Reference
Cross Section cm	Material							
3·5 diam.	brass	air	air	760	1.04–1.4	0–0·01	4·5	Emrich and Curtis
0·64 × 7·6	duraluminum	air	air	760	1·04–1·4	0·004–0·03	4·5	Emrich and Curtis
15 diam.	—	air	air	—	1–1·2	0–0·002	—	Emrich and Harrison
0·64 × 7·6	glass	air	air	760	1·14–1·33	0·04–0·02	0·5	Hoover
15 diam.	—	H_2	air	38	8	0·009	33	Spence and Woods
9·5 diam.	stainless steel	H_2, He	air	5–100	5–10	0·005–0·01	30	Jones
7·6 × 7·6	steel	air	air	0·8–29	3·1–2·4	0·03	2·3	Boyer
2·5 diam.	—	double diaphragm He or combustion driven	air	0·5–5	10–20	0·05	5	Schexnayder
15 diam.	aluminum and glass	He heated by arc discharge	air	0·1–1	17–30	0·03	5	Camm and Rose
61 diam.	stainless steel	combustion of H_2-O_2-N_2 mixture	air	0·02	14–24	0–0·007	10	Lin and Fyfe
5·1 × 18	steel	H_2	N_2	9·5–3·8	2·5–3·2	0·05	3·7	Hollyer
5·1 × 18	steel	H_2	N_2	37–15	2·5–3·3	0·06–0·08	3·7	" "lyer
5·1 × 5·1	steel	H_2	N_2	5	9	0·026	5·5	w ldron
5·1 × 5·1	steel	H_2, O_2, He constant volume burning	N_2	25	10	0·043	5·5	Waldron

5·1 × 5·1	steel	H_2, O_2, He self ignition	N_2	25	8	0·082	5·5	Waldron
5·1 × 5·1	steel	H_2, O_2, He detonation	N_2	25	13	0·11	5·5	Waldron
5·1 diam	glass	H_2	N_2	0·6–15	4–9	0·1–6·02	2	Toennies
5·2 diam	Monel	He	Ar	10	7	0·045	2	Wray
5·1 diam	glass	H_2	Ar	0·6–100	4–8	0·1–0·01	2	Toennies
10 diam	brass	He	Xe-O_2	10–30	6–8	0·01		Rink, Knight and Duff
2·5 diam	glass	H_2	Br_2	2–80	5	0·02	1	Palmer and Hornig
7·6 diam	glass	H_2	C_2H_2	2–60	3–8	0 ± 0·02	1·3	Aten

Aten, C. F., unpublished

Beyer, D. W., Univ. of Toronto, Inst. of Aerophysics Tech. No. 8 (1956), *Effects of Kinematic Viscosity and Wave Speed on Shock Wave Attenuation.*

Camm, J. C. and Rose, P. H., *Phys. Fluids*, **6**, 663 (1963).

Emrich, R. J. and Curtis, C. W., *J. Appl. Phys.*, **24**, 360 (1953).

Emrich, R. J. and Harrison, F. B., *Phys. Rev.*, **73**, 1225 (1948).

Hollyer, R. N. Jr., Univ. of Michigan, Engineering Research Institute (1953). *A Study of Attenuation in the Shock Tube.*

Hoover, H. L., Lehigh University Institute of Research, *Measurement by Timed Spark Shadow Graphs of Shock Velocities in the Shock Tube.*

Jones, J. J., *Nat. Advisory Comm. Aeronaut. Tech. Note* 4072 (1957).

Lin, S. C. and Fyfe, W. I., *Phys. Fluids*, **4**, 238 (1961).

Palmer, H. B. and Hornig, D. F., *J. Chem. Phys.*, **26**, 95 (1957).

Rink, J. P., Knight, H. T. and Duff, R. E., *J. Chem. Phys.*, **34**, 1942 (1961).

Scheuyder, C. J. Jr., *J. Aero/Space Sci.*, **25**, 527 (1958).

Spence, D. A. and Woods, B. A., in *Hypersonic Flow*, Collar, A. R. and Tinkler, J., ed. Butterworths, London (1960).

Toennies, J. P., unpublished.

Waldron, H. F., *Univ. of Toronto, Inst. of Aerophys. Report No.* 50 (1958), *J. Aeronaut. Sci.*, **25**, 719 (1958).

Wray, K. L., *Dissertation*, Brown University (1955).

where x is the distance from the diaphragm, D the hydraulic diameter (4 times the ratio of area to perimeter of the cross section) and $\bar{I}$ the attenuation coefficient which has values between $0{\cdot}6 \times 10^{-2}$ and $1{\cdot}0 \times 10^{-2}$ in their examples. Although $\bar{I}$ may be expected to depend on p_1/p_2, γ, and D, significant correlations are hard to establish from these data.

In addition to velocity attenuation other evidence of wall action from the walls comes from measurements of shock curvature and of pressure and density changes behind the front. For shocks of $M_1 \approx 2$ ($p_1/p_1 = 50$) in nitrogen (3·5 cm diameter shock tube, measuring station 3 m from diaphragm) at $p_1 = 1/10$ atm measurements showed an increase of density, ρ_2, of about 5% per msec in the hot gas behind the shock.[3] The increase was less rapid at greater distances from the diaphragm. Pressure measurement in the same tube were not precise, and although some increase may have occurred with time in the hot gas, the change was smaller than the experimental error.[2] In another investigation[3] in a tube of 7·6 cm square cross section a decrease in pressure of approximately 1% per millisecond was noted ($p_1 = 1$ atm air, $p_2/p_1 = 1{\cdot}5$). A small increase in pressure behind the shock was observed by Trimpi and Cohen from measurements of the displacement of a thin diaphragm. ($\Delta(p_2 - p_1)$ approximately 5% per msec for $M_1 \approx 2$ in air).[4]

Because in Mack's experiments the density was measured with an interferometer observing through the boundary layers on the windows, some of the rise may have been due to an increased thickness of the cold layers. This is consistent with other experiments on shocks in Br_2 which showed a constant density within 1% for 100 μsec behind the shock followed by a small increase attributed to boundary layer thickening.[5] This effect also must contribute to the substantial rise in density observed by Duff[6] in his experiments in a 2·86 cm diameter tube with low pressure shocks in argon using an electron beam densitometer. He observed $[\Delta\rho_2/(\rho_2 - \rho_1)] \simeq 0{\cdot}5$ at approximately 100 mm behind a shock of $M_1 = 1{\cdot}6$ with $p_1 = 0{\cdot}5$ mm. Density and pressure measurements have been made by Rose and Nelson in the Mach number range 6–20 for shocks in air with initial pressures from 1·0–40 cm.[7] The same general behavior was observed as found by others for weaker shocks.

1. Mack, J. E., *Density Measurement in Shock Tube Flow with the Chronointerferometer*, Inst. of Research, Lehigh University (1954).
2. Emrich, R. J. and Peterson, R. L., *Pressure Variation with Time in the Shock Tube*, Inst. of Research, Lehigh University (1956).
3. Huber, P. W., Fitton, C. E. Jr. and Delpino, F., *Nat. Advisory Comm. Aeronaut. Tech. Note* 1903 (1949).
4. Trimpi, R. L. and Cohen, N. B., *Nat. Advisory Comm. Aeronaut. Tech. Note* 3375 (1955).
5. Palmer, H. B., *J. Appl. Phys.*, 27, 1105 (1956).
6. Duff, R. E. *Phys. Fluids*, 2, 207 (1959).
7. Rose, P. H. and Nelson, W., *On the Effect of Attenuation on Gas Dynamic Measurements Made in Shock Tubes*, AVCO Everett Research Report 24 (1958).

4. Relation of diaphragm pressure ratio (p_4/p_1) to shock pressure ratio (p_2/p_1)

In order to have continuity of p and $u_1 - u_2$ across the contact surface, the shock moving into the low pressure gas must accelerate and compress this gas to the same conditions of p and $u_1 - u_2$ produced by the expansion of the gas originally in the high pressure section. This additional relation means that for a given shock (fixed p_2, $u_1 - u_2$) and a specified driver gas (fixed γ_4) there is only one possible value of the pressure, p_4, in the high pressure section of the shock tube. Several authors[1] have derived the relation between p_4/p_1 and p_2/p_1 for the case of ideal gases and constant specific heats. This is done by eliminating $u_1 - u_2$ from Equation 5.2 and Equations 2.28 and 30. The result is

$$\frac{p_4}{p_1} = \frac{p_2}{p_1}\left[1 - \frac{a_1(\gamma_4 - 1)\left(\frac{p_2}{p_1} - 1\right)}{a_4(\gamma_4 - 1)\sqrt{\frac{2\gamma_1}{\gamma_1 - 1}\frac{p_2}{p_1}\left(\frac{\gamma_1 - 1}{\gamma_1 - 1} + \frac{p_1}{p_2}\right)}}\right]^{-(2\gamma_4)/(\gamma_4 - 1)} \qquad \ldots 5.3$$

There are several important conclusions to be drawn from this result. For a given p_2 and p_1 the higher the ratio of sound velocities, a_4/a_1, and the larger the γ_1 the stronger is the shock which is formed. The solid lines in Figs. 5.8, 5.9, and 5.10 show the p_4/p_1 required by Equations 5.3 and 2.28 to produce a given M_s for shocks in argon, nitrogen and acetylene (constant γ_1) respectively when 3 different gases H_2, He and Ar are used in the high pressure section. It is clear that H_2 and He produce much stronger shocks for a given p_4/p_1. This is mostly because of their low molecular weight and consequently high sound velocity. H_2 is more effective than He but is sometimes to be avoided if it may react with the gas in the low pressure section. There is a limiting value of p_2/p_1 as p_4/p_1 increases. This limit corresponds to the vanishing of the expression in the bracket in Equation 5.3.

When Equation 5.3 does not apply because the specific heats of the gases vary, the calculation of p_4/p_1 is somewhat more tedious but still quite feasible. In the high pressure section the expansion for strong shocks, an almost free expansion, cools the gas so much that condensation can occur; if the gas is hydrogen the heat capacity decreases because the rotational degrees of freedom are no longer fully excited as is the case at room temperature where c_v is $\frac{5}{2}R$. In this case Equation 5.1 may be integrated either numerically or with an analytical expression for $c_v(T)$ to give the flow velocity achieved when H_2 is expanded from p_4 to p_2.[2] Since only the ratio p_4/p_2 is needed the results may be used for H_2 driver gas in combination with any gas in the low pressure section to predict shock strengths as a function of p_4/p_1. It is only necessary to calculate p_2/p_1 and $u_1 - u_2$ for the desired shock wave in

1. Kobes, K., *Z. österr. Ing. u. Architekt. Ver.* 62, 533 (1910).
   Schardin, H., *Physik. Z.*, 33, 61 (1932).
   Taub, A. H., (in Bleakney, Weimer and Fletcher, *Rev. Sci. Instr.* 20, 814 (1949)).
   Payman, W. and Shepherd, W. C. F., *Proc. Roy. Soc.* **A186**, 293 (1946).
2. Duff, R. E., *The Use of Real Gases in a Shock Tube*, Univ. of Michigan, Engineering Research Inst. Report (1951).

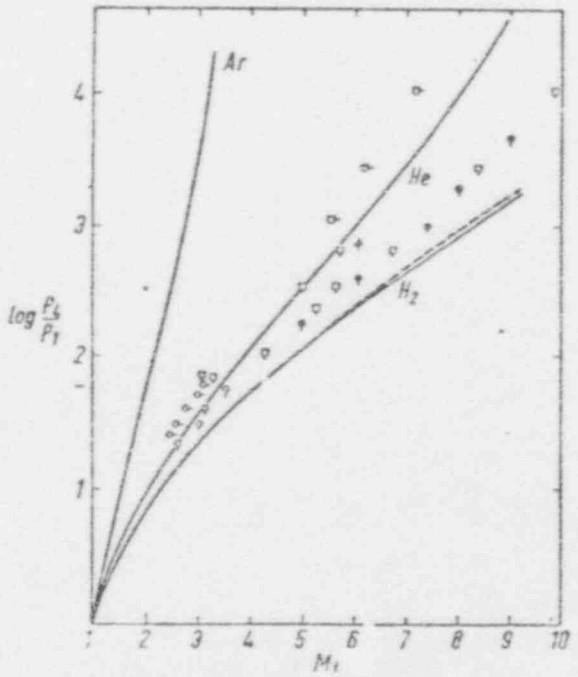

FIG. 5.8. $\log p_4/p_1$ vs. Mach number for shock waves in argon. Various gases in the high pressure section (driver section). $T_1 = 300°K$. Experimental points described in Table 5.3. Curves calculated from Eq. 5.3 constant γ (solid) and $\gamma(T)$ (dotted).

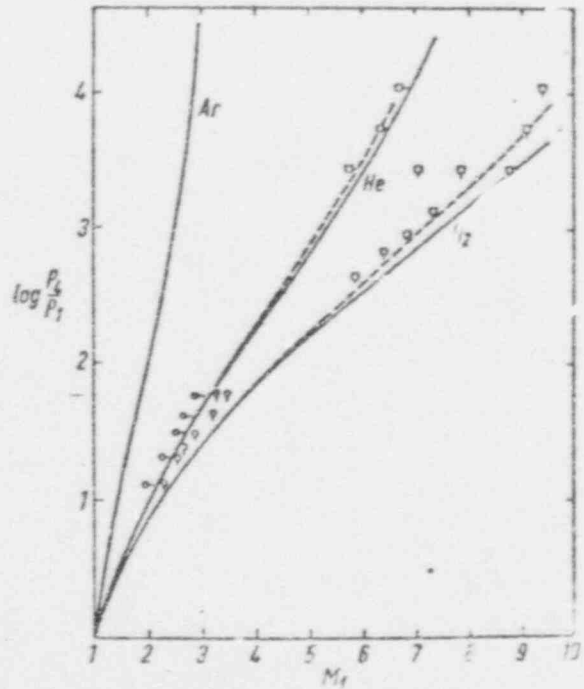

FIG. 5.9. $\log p_4/p_1$ vs. Mach number for shock waves in nitrogen. Various driver gases. $T_1 = 300°K$. Experimental points described in Table 5.3. Curves calculated from Eq. 5.3 constant γ (solid) and $\gamma(T)$ (dotted).

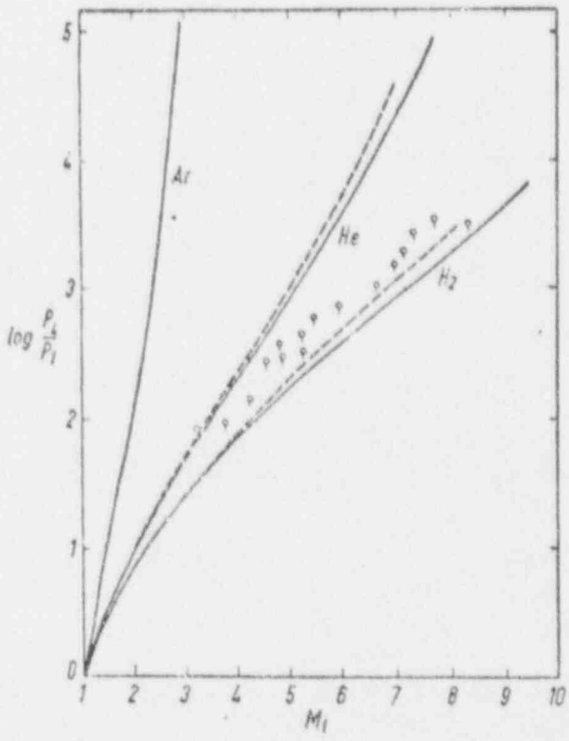

FIG. 5.10. $\log p_4/p_1$ vs. Mach number for shock waves in acetylene. Various driver gases. $T_1 = 300$ K. Experimental points described in Table 5.3. Curves calculated from Eq. 5.3, constant γ (solid) and $\gamma(T)$ (dotted)

the gas to be heated; and then, for this $u_1 - u_2$ to calculate the ratio p_4/p_2 which gives p_4/p_1 directly. For monatomic gases Equation 5.2 is satisfactory until the onset of condensation, which is not a problem with He.

When the gas in the low pressure section is not ideal or not of constant heat capacity, p_2 and $u_1 - u_2$ must be calculated as functions of M_1 or p_2/p_1 by the methods outlined in Chapter 3 for real gases. Then the desired p_4/p_1 can be found as before by matching the values of $u_1 - u_2$. Table 5.2 shows the values of p_4/p_2 required to produce various $u_1 - u_2$ for He and H_2 (constant $c_v = \frac{3}{2}R$ and $c_v = c_v(T)$[1]). Figure 5.8, 5.9 and 5.10 also show (dotted lines) curves for H_2 and He driven Ar, N_2, and C_2H_2 shocks using experimental heat capacities for all the gases. Some experimental measurements are included for comparison (see Table 5.3).[2]

1. Farkas, A., *Orthohydrogen, Parahydrogen and Heavy Hydrogen*, Cambridge Univ. Press, Cambridge (1935) p. 19.
2. For experimental results see also Jones, J. J., *Nat. Advisory Comm. Aeronaut. Tech. Note* 4072 (1957).

TABLE 5.2

Flow Speeds and Temperatures Produced by Expansions of H_2 *and* He *Driver Gas. Initial Conditions are Stationary Gas at* 300°K.

	H_2 $c_v = \frac{5}{2}R$		H_2 $c_v = c_v(T)$		He $c_v = \frac{3}{2}R$	
T°K	p_4/p_1	$u_1 - u_2$ mm/μsec	p_4/p_1	$u_1 - u_2$ mm/μsec	p_4/p_1	$u_1 - u_2$ mm/μsec
300	1	0	1	0	1	0
275	1·356	0·280	1·338	0·276	1·24	0·130
250	1·983	0·573	1·856	0·562	1·58	0·266
225	2·74	0·882	2·65	0·858	2·05	0·410
200	4·13	1·208	3·92	1·164	2·76	0·561
175	6·60	1·555	6·04	1·479	3·85	0·722
150	11·31	1·927	9·77	1·804	5·66	0·895
125	21·4	2·33	16·80	2·14	8·92	1·084
100	46·8	2·78	31·5	2·48	15·59	1·292
75	128·0	3·29	67·2	2·84	32·0	1·529
50	529·	3·89	189·6	3·24	88·2	1·809
40	1155·	4·18	332·	3·43	154·1	1·941
30	3160·	4·50	685·	3·64	316·	2·09
25	5990·	4·68	1008·	3·76	499·	2·18
20	13070·	4·88	1897·	3·89	871·	2·27

In general for a given shock velocity the agreement of experimental p_4/p_1 with that calculated is within a few percent for shocks with $M_1 < 1.5$ but falls off so that at $M_1 = 5$–10 the calculated values are only approximately one half the experimentally required ones. In spite of this discrepancy the calculated curve is very useful for interpolating between experimental points.

5. Methods of increasing the strength of shock waves produced in shock tubes

Resler, Lin, and Kantrowitz[1] have considered various methods of obtaining stronger shocks than those calculated from Equation 5.3 with the driver gas at room temperature. These methods fall into two groups, the first of which involves increasing the sound speed of the driver gas, a_4. This may be done by heating the gas in several ways. Effective external heating of the high pressure section is usually awkward, but internal heating by solid heating elements can be useful. Better still is heating by an electrical discharge[2] or by internal combustion. A common procedure is to use a H_2 driver gas which contains a small amount of O_2 and then to ignite the mixture just before the diaphragm is broken. For 12% O_2 the sound speed in the heated gas is about 1.67 times that for pure H_2 at room temperature and in a typical case this led

1. Resler, E. L., Lin, S. C. and Kantrowitz, A., *J. Appl. Phys.* 23, 1390 (1952).
2. Camm, J. C. and Rose, P. H., *Phys. Fluids*, 6, 663 (1963).

TABLE 5.3

Data for Experimental Points on Bursting Pressure vs. M_s, Figures 5.8, 9, 10

Symbol	Driver Gas	Heated Gas	Distance from Diaphragm	Range of P_1	Shock Tube	Reference
○	H_2	Ar	3·2 m	50–90 mm	5·1 × 18 cm steel	Hollyer, Univ. of Michigan, Engineering Research Institute Report, 1953
○	He	Ar	3·2 m	60–90 mm	5·1 × 18 cm steel	Hollyer, Univ. of Michigan, Engineering Research Institute Report, 1953
●	H_2	Ar	—	10–150 mm	3·8 cm diam. steel or brass	Resler, Lin, Kantrowitz, *J. Appl. Phys.*, 32, 1390 (1952)
□	H_2	Ar	2 m	0·6–180 mm	5 cm diam. glass	J. P. Toennies unpublished
□	He	Ar	2 m	0·6–6	5 cm diam. glass	J. P. Toennies unpublished
△	H_2	Ar	2 m	9	2·5 cm diam. glass	J. P. Toennies unpublished
○	H_2	N_2	3·2 m	15–150 mm	5·1 × 18 cm steel	Hollyer, Univ. of Michigan, Engineering Research Institute Report 1953
○	He	N_2	3·2 m	35–70 mm	5·1 × 18 cm steel	Hollyer, Univ. of Michigan, Engineering Research Institute Report 1953
□	H_2	N_2	2 m	0·6–15 mm	5·1 cm diam. glass	J. P. Toennies unpublished
□	He	N_2	2 m	0·6–2·4 mm	5·1 cm diam. glass	J. P. Toennies unpublished
○	H_2	C_2H_2	1·5 m	2–60 mm	7·6 cm diam. glass	C. F. Aten unpublished

ATTACHMENT #2

ADVANCES IN APPLIED MECHANICS

Editors

H. L. DRYDEN TH. VON KÁRMÁN

Managing Editor

G. KUERTI

Case Institute of Technology, Cleveland, Ohio

Associate Editors

F. H. VAN DEN DUNGEN L. HOWARTH J. PÉRÈS

VOLUME VI

1960

ACADEMIC PRESS NEW YORK AND LONDON

The Propagation of Shock Waves along Ducts of Varying Cross Section

By W. CHESTER

University of Bristol, Bristol, England

NOTATION

A	Cross-sectional area of the duct
a	Sonic speed
B	See equation (3.33)
C_+, C_-	Characteristics
d	Distance travelled by shock
F, G, H	See equations (3.25), (3.26), (3.27)
I	See equation (3.5)
K, K_0	See equations (3.2), (3.10)
M	Mach number
P	Characteristic
p	Pressure
q	Fluid speed
R	See equation (3.6)

r	Radial co-ordinate
t	Time
U	Shock velocity
x	Co-ordinate along the axis of the duct
z	Pressure ratio across the shock
α, β	See equations (3.10), (3.11)
γ	Adiabatic index
$1 + \delta$	Mach number of weak shock
$1 + \epsilon$	Mach number of the flow ahead of the shock
η	See equation (3.14)
λ	See equation (3.32)
μ	See equation (3.3)
ρ	Density
ν	See equation (3.38)

Subscripts:

c	Characteristic quantity
d	Flow quantities downstream of area change
i	Incident shock
r	Reflected shock
t	Transmitted shock
T	Stagnation conditions
u	Flow quantities upstream of area change
$1 - 5$	Except for Section V these subscripts refer to the regions of flow shown in Figs. 2 and 3. In Section V subscripts 1 and 2 refer respectively to flow quantities immediately in front of, and immediately behind, the shock

I. General Introduction

When a shock wave travels along a duct whose cross section changes continuously, there is an interaction between the shock and the changing cross section. The flow behind the shock is disturbed and there is a modification of the shock strength. A number of writers have considered the effect of the interaction on the flow behind the shock; this work has been noted in the bibliography and reference is made to some of it in the following pages. The present article will, however, mainly consider the modifying effect on the shock wave itself. This problem is of particular interest, not least because of the success of the relatively simple techniques which have been evolved to deal with it.

By way of introduction consider the propagation of a shock wave between two walls of infinite extent, forming a two-dimensional channel of uniform width connected to a channel of uniformly increasing width. As the shock passes into the diverging section two independent diffracted pulses are produced, one at each corner (Fig. 1). Eventually, as the pattern expands, the two pulses will interact and suffer repeated reflection from the two walls. The whole process is too complex to attempt a complete mathematical description, but if the angle of divergence is small the problem becomes a

linear one. The interaction of the pulses can then be replaced by a simple superposition and the effect on reflection of the small divergence of the walls can be ignored, for this will be of the second order for a pulse in which the perturbation is already small. The diffraction problem for a single corner was solved by Lighthill [1], and the image system which simulates repeated reflection between two walls was studied by Chester [2]. Furthermore, since the problem is linear, the solution for arbitrary (though small) variations in channel width can be obtained by summation over all the elementary variations in slope. Thus if the channel consists of two sections of uniform width joined by a transition section of finite length the asymptotic behaviour of the flow can be deduced, and consists essentially of a uniform but modified transmitted shock and a plane reflected pulse. The theory of shock propagation described in Section III stems from the solution of this problem.

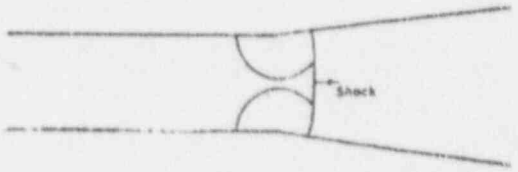

FIG. 1. The diffraction pattern produced by the interaction of a shock wave with a diverging channel.

Freeman [3] has also investigated the image system in the problem of the last paragraph and has deduced therefrom that the perturbations behind the shock are oscillatory in character and decay asymptotically like $d^{-3/2}$, where d is the distance travelled by the shock wave from the transition producing the perturbations. Freeman also shows that the rate at which the perturbations decay depends, in addition, on the strength of the shock, being strongest when the shock Mach number is about 1.15 and decreasing sharply for both strong and weak shocks.

Another simple example which serves to introduce the subject matter of this review is the problem of an acoustic pulse travelling along a tube of varying cross section. This is again a linear problem because the weak shock can only produce a small disturbance. The restriction to small variations in cross-sectional area is, however, no longer necessary. Here two interesting cases arise, both of which are discussed by Rayleigh [4]. The first is that of a sharp fronted pulse proceeding along a duct for which the cross section varies continuously. At the front of the pulse the energy reflected is negligible on a linear theory, so that the transmitted energy is invariant. Since the latter is proportional to the square of the amplitude multiplied by the cross section, it follows that the amplitude varies inversely as the square root of the cross section. The result is *not* true in the rear part

of the disturbance because the second order effects may accumulate to a significant modification over a finite change of cross section. But this integrated effect cannot modify the front of the pulse since disturbances to the rear travel no faster than the front itself. Such disturbances therefore never reach the front.

The other case is the problem of reflection and transmission at an abrupt change in cross section. Here the argument of the previous paragraph is no longer valid, for a significant proportion of energy will now be reflected by the discontinuity even at the head of the wave. But a simple argument gives the ultimate behaviour of the transmitted and reflected pulses. Let the cross section change discontinuously from A_2 to A_1 and let the Mach numbers of the incident, reflected, and transmitted pulses be respectively $(1 + \delta_i)$, $(1 + \delta_r)$ and $(1 + \delta_t)$. Then continuity of pressure and mass flux demands that

$$\delta_i + \delta_r = \delta_t, \tag{1.1}$$

$$A_2(\delta_i - \delta_r) = A_1\delta_t, \tag{1.2}$$

since the perturbations in flow velocity and pressure are proportional to δ on a linear theory. These equations imply that

$$\frac{\delta_t}{\delta_i} = \frac{2A_2}{A_1 + A_2} \tag{1.3}$$

which agrees with the previous result only when $|A_2 - A_1| \ll A_2$*.

These solutions for the acoustic pulse illustrate two extreme situations in the problem of shock propagation along ducts. In the first the interactions behind the front of the pulse have no effect whatever on the front itself. In the second they are allowed to exert their utmost effect.

For a shock wave of finite strength travelling along a duct whose cross section varies continuously, but by a significant fraction of itself, the answer lies somewhere beteeen these two extremes. The disturbances created behind the shock front will now be continually overtaking the shock with consequent modification of its strength. If these effects continue to be ignored, notwithstanding the lack of rigorous justification, a simple solution can be obtained which has been studied in detail, originally by Chisnell [5] and later by Whitham [6, 7]. This theory is the main theme of Section III, and evidence is offered which suggests that Chisnell's hypothesis is sound and in certain circumstances predicts the variation in strength of the shock wave, as it progresses, to good accuracy.

---

* The subscripts have been chosen to be consistent with the numbering of the various flow regions in Figs. 2 and 3, and hence with later equations which refer to more general models. Note that the subscript 2 refers to the *upstream* part of the duct, and the subscript 1 to the *downstream* part.

On the other hand, suppose the duct consists of two uniform sections connected by a transition section of finite length. The shock is then initially of uniform strength in the upstream section. Ultimately it tends to become a shock wave of uniform (though different) strength in the downstream section. When this happens the modifying effects of the disturbances produced by the change in cross section will have been completed, and the only non-steadiness will be the continual growth of the uniform region behind the shock. This is the generalization of the second of the acoustic problems. The model has been used by Kahane, Warren, Griffith and Marino [8], Laporte [9] and Parks [10]. It is described in Section II.

It is naturally of interest to compare the two theories directly, and this is done in Section IV. Such a comparison gives some idea of the extent to which upstream disturbances are capable of modifying the shock strength. However it should be pointed out that, in application, they are meant to describe different situations. Chisnell intended that his solution should be used only to describe the progressive modification of a shock as it travelled along a duct whose cross section varied 'not too rapidly'. On the other hand, the method of Section II gives the ultimate strength, when the shock has again become uniform, after passing through a transition section of finite length.

Section V contains some previously unpublished results obtained by extending the ideas of the previous sections to deal with the progress of a shock wave along a duct in which a steady flow is already established. There it is found, for example, that the pressure difference across the shock has a maximum where the steady flow is subsonic, the precise cross section depending on the shock strength.

The behaviour of a weak disturbance facing upstream, in the neighbourhood of a sonic throat, is also deducible from the theory of Section V. It is shown that if such a disturbance is initially moving upstream it continues to do so and decreases in strength. If it is initially moving downstream it continues in that direction, but its strength may increase or decrease.

II. The Steady-State Theory

1. *Discussion of the Model*

In the theory described here the channel will always consist of two sections, each of uniform cross-sectional area, joined by a transition section of finite length. Only the ultimate flow will be considered, when conditions behind the shock are independent of the time and the shock itself is moving along the downstream section with uniform speed and strength.

To set up a model which describes such a flow it would seem natural to generalise the argument used for an acoustic pulse. This would imply a

transmitted shock wave, and a reflected shock wave or rarefaction wave according as the transition is a contraction or expansion. The flow between the two waves would follow the known behaviour for steady flow in a duct

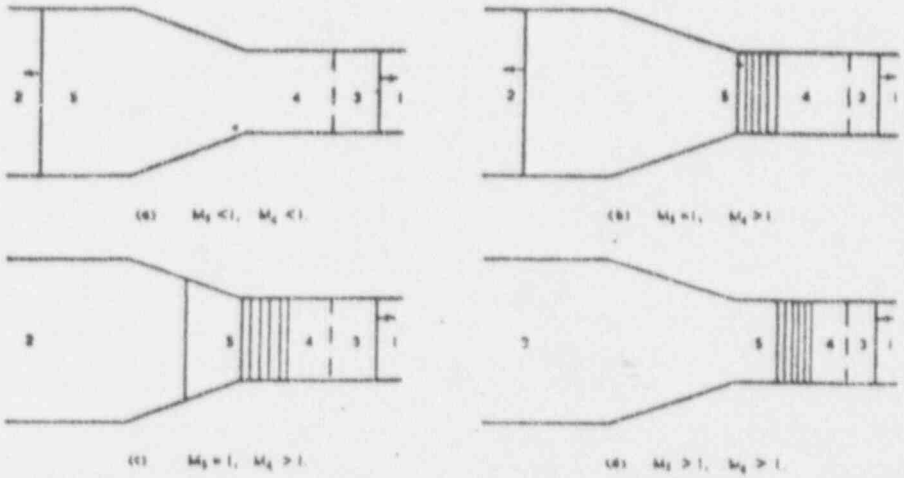

FIG. 2. Interaction of a shock wave with a contraction; steady state theory.

Such a model, however, is not sufficiently flexible in the general case, and will not allow the transition relations across the two waves to be satisfied simultaneously with the relations which the flow must satisfy through the area change. It is in fact necessary to include a contact discontinuity in the downstream section. The necessary matching of the different parts of the flow is then possible. The existence of such a discontinuity is well supported by experimental evidence.

The above argument suggest the models pictured in Figs. 2(a) and 3(a) for a contraction and an expansion respectively. But these two models are still not sufficient to cover the whole range of possibilities. Thus for a contraction it is not possible to exceed unit Mach number immediately downstream of the contraction if the upstream flow is subsonic, and calculations show that for sufficiently strong shock waves the model shown in Fig. 2(a) is not consistent with this fact. Laporte [9] proposes model 2(b) in such cases. Here a simple wave begins at the end of the contraction, where sonic velocity is just reached. Supersonic flow upstream of the transmitted shock is then achieved through this expansion wave. Of course, it is possible for supersonic flow to exist behind the incident shock, and for this flow to remain supersonic even after the contraction. Then no reflected disturbance is produced which is strong enough to move upstream. In addition to the transmitted shock and the contact discontinuity, this situation is completed by an expansion wave facing upstream, but convected

downstream as in Fig. 2(d). Fig. 2(c) illustrates an intermediate case in which a stationary shock wave appears in the transition section itself. The situation in the downstream section is qualitatively similar to that in Fig. (2b).

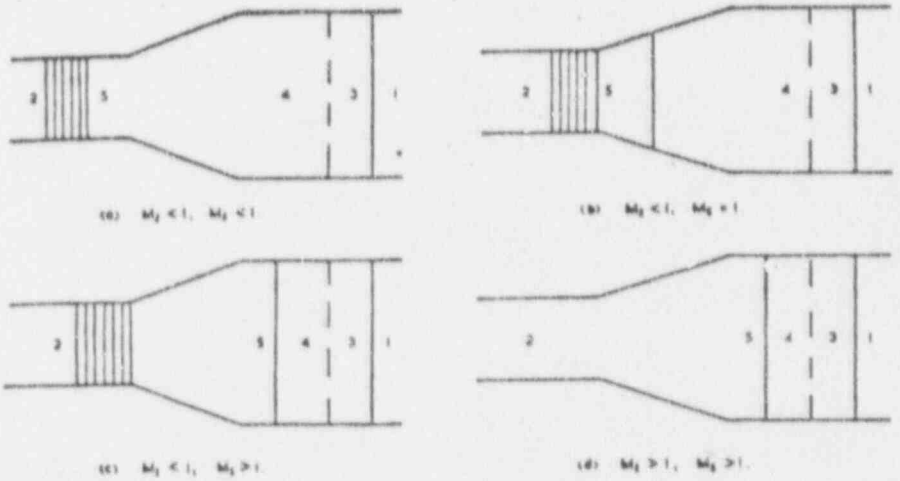

FIG. 3. Interaction of a shock wave with an expansion; steady state theory.

The corresponding possibilities in the flow through an expansion are shown in Fig. 3. For incident shock strengths below a certain critical value, the model differs from Fig. 2(a) only in that a rarefaction wave is reflected instead of a shock. As the strength of the incident shock increases, the Mach number of the flow downstream of the reflected wave also increases until finally it becomes sonic at the beginning of the expansion, and supersonic by further expansion until it reaches a stationary shock wave. Beyond this shock the flow remains subsonic [Fig. 2(b)]. For stronger incident shocks the stationary shock moves out of the transition section and is convected downstream [Fig. 2(c)]. Finally the expansion wave in the upstream section can disappear entirely giving Fig. 2(d).

Not all of the flow regimes which have been described are necessarily attainable for any given transition. For example, that shown in Fig. 2(c) will first appear when the incident shock is just strong enough to produce a reflected shock which remains stationary at the upstream end of the transition section. Let the Mach numbers upstream and downstream of such a stationary shock be M_2 and M_* respectively. Then, by the shock transition relations

$$M_*^2 = \frac{(\gamma - 1)M_2^2 + 2}{2\gamma M_2^2 - (\gamma - 1)} \tag{2.1}$$

where γ is the adiabatic index. It follows that M_* is a monotonic decreasing function of M_2. Since M_2 cannot exceed $\{2/\gamma(\gamma - 1)\}^{1/2}$, which is the limiting

value of M_1 as the strength of the incident shock tends to infinity, (2.1) implies that

$$M_e^2 > \frac{2(\gamma-1)}{\gamma(3-\gamma)}. \tag{2.2}$$

Now the area, Mach-number relation for steady flow through the contraction is

$$\frac{A_2}{A_1} = \frac{M_2}{M_e}\left\{\frac{2+(\gamma-1)M_e^2}{2+(\gamma-1)M_2^2}\right\}^{\frac{(\gamma+1)}{2(\gamma-1)}}, \tag{2.3}$$

where M_2 is the Mach number at the downstream end of the transition section and must satisfy the inequality $M_2 \leqslant 1$. It follows that the maximum contraction which allows the possibility of model 2(c) is given by (2.3) with $M_e = \{2(\gamma-1)/\gamma(3-\gamma)\}^{1/2}$ and $M_2 = 1$. This gives

$$\begin{aligned} A_2/A_1 &= (\gamma-1)^{-1/2}\{2/\gamma(3-\gamma)\}^{\frac{1}{\gamma-1}}, \\ &= 1.191 \quad \text{for} \quad \gamma = 7/5, \\ &= 1.046 \quad \text{for} \quad \gamma = 5/3. \end{aligned} \tag{2.4}$$

For contraction ratios which exceed this value, models 2(a) and 2(b) appear to cover the whole range of incident shock strengths, and there is always some upstream influence.

It is, however, interesting that the critical condition for model 2(d) is slightly less restrictive than (2.4). For this model the area, Mach-number relation for steady flow through the transition section is similar to (2.3) but with M_e replaced by M_1. Substitution of the limiting value of M_1, namely $\{2/\gamma(\gamma-1)\}^{1/2}$, in this relation, together with $M_2 = 1$, gives

$$\begin{aligned} A_2/A_1 &= (\gamma-1)^{1/2}(2/\gamma)^{\frac{1}{\gamma-1}}, \\ &= 1.543 \quad \text{for} \quad \gamma = 7/5, \\ &= 1.073 \quad \text{for} \quad \gamma = 5/3. \end{aligned} \tag{2.5}$$

The implication is that under certain conditions there are two possibilities, 2(b) or 2(d). In practice it is probable that 2(b) will prevail; if it does not there is certainly no continuous transition from 2(b) to 2(d) unless the contraction ratio is less than the value given by (2.4).

The various models contained in Figs. 2 and 3 seem to cover all the possibilities for a monotonic area change apart from minor modifications (for example, in the expansion it is possible for the reflected wave to disappear before the stationary shock has passed into the downstream

section). They are also calculable from, and consistent with, the initial conditions and the known physical limitations for such flows.

The procedure for calculating the strength of the transmitted shock is illustrated by taking model 2(a) as a typical example. The flow in region 2 is that produced behind the incident shock, and is therefore calculable in terms of the strength of that shock, the transition relations which hold across it, and conditions in region 1. Similarly the flow in region 5 depends on that in region 2 and one other parameter — say the strength of the transmitted shock. The flow in region 4, which is deducible from that in region 5 and the relations for steady flow through a duct, is also dependent on this parameter. By its elimination, a relation can be obtained connecting the pressure and velocity in region 4. Since the pressure and velocity are continuous through the contact discontinuity, this relation persists in region 3. Together with the known flow ahead of it, this is just sufficient information to determine the strength of the transmitted shock. The actual computation requires the use of simple numerical techniques. The details are omitted.

2. *Discussion of the Results*

The results of some numerical calculations are shown in Figs. 4–7. Fig. 4 was constructed from calculations made by Laporte [9] for contraction ratios of 2 : 1, 5 : 1 and ∞ : 1, and a value of 5/3 for the adiabatic index. It shows the variation of the ratio of the pressure differences across the transmitted and incident shocks with the Mach number of the incident shock.* Fig. 4 also shows the asymptotic values for strong shocks, and the tangent to the curve at the weak shock end of the scale. The latter is obtained from model 2(a), or 3(a), by expanding all the flow variables as power series in the strength of the incident shock. The first three terms are given by

$$\frac{A_1 + A_2}{2A_2} \cdot \frac{p_3 - p_1}{p_2 - p_1} = 1 - \frac{3 - \gamma}{4\gamma} \cdot \frac{1 - A_1/A_2}{1 + A_1/A_2} \cdot (z - 1) + \frac{(\gamma + 1)^2}{8\gamma^2} \frac{1 - A_1/A_2}{(1 + A_1/A_2)^2} \left\{ \frac{2}{\gamma + 1} (3 + 2A_1/A_2) - \frac{1}{4} (4 + 3A_1/A_2) + \left[\frac{(1 - A_1/A_2)^2}{(1 + A_1/A_2)} \left(\frac{1}{3(\gamma + 1)} - \frac{1}{8} \right) \right] \right\} (z - 1)^2, \tag{2.6}$$

* The pressure difference across the shock, rather than the pressure ratio, has been chosen as a measure of its strength since the ratio is unsuitable for weak shocks. The Mach number of the incident shock is, however, used as the abscissa, because it gives more prominence than the pressure difference to that part of the curve which describes the weaker shocks. This is where most of the variation takes place. There is, of course, a simple relation, (2.7), between Mach number and pressure difference.

where

$$s - 1 = p_2/p_1 - 1 = \frac{2\gamma}{\gamma + 1}(M^2 - 1), \tag{2.7}$$

and the term in square brackets is to be included only for an expansion, i.e. $A_2 < A_1$. In these equations $(p_3 - p_1)$ and $(p_2 - p_1)$ are respectively the pressure differences across the transmitted and incident shocks, and M is the Mach number of the latter.

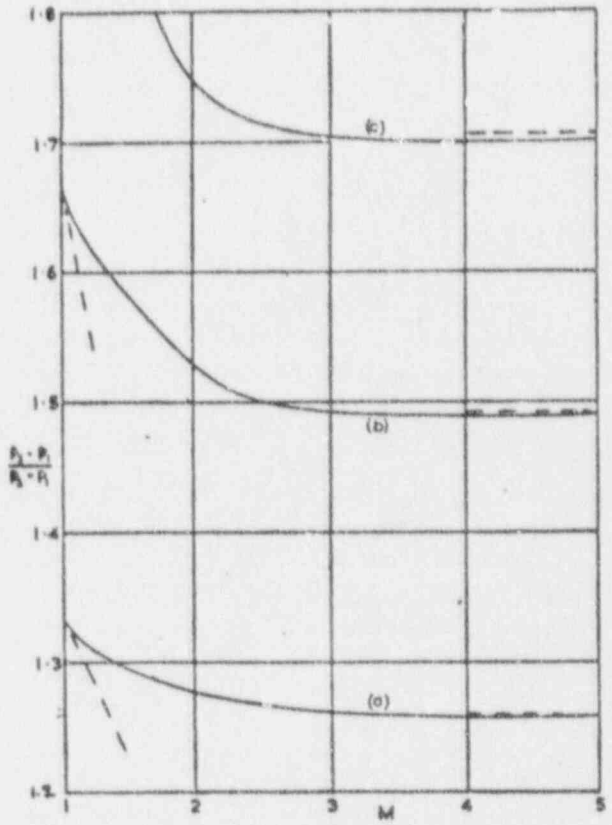

FIG. 4. The ratio of the pressure differences across the transmitted and incident shocks as a function of the Mach number of the incident shock; steady state theory. (a) $\gamma = 5/3$ and 2 : 1 contraction ratio; (b) $\gamma = 5/3$ and 5 : 1 contraction ratio; (c) $\gamma = 5/3$ and ∞ : 1 contraction ratio.

The contraction and expansion have different analytical expressions for the third term in (2.6) because of the entropy change (which is of the

third order in the pressure difference) across the shock reflected by a contraction. Actually the difference is zero for $\gamma = 5/3$ and quite small for $\gamma = 7.5$.

Reference to Fig. 4 shows that the series in (2.6) converges slowly except for very weak shocks. Even for a 2 : 1 contraction the tangent (obtained from the first two terms of (2.6)] very quickly ceases to be a reliable approximation. The addition of another term improves the approximation as far as $M = 1.1$. Beyond this it overestimates and even gives the wrong trend – the right hand side of (2.6) has a minimum at roughly this value of M. For stronger contractions the convergence is still slower, and the series solution fails completely for very large contraction ratios.

Fig. 4(c) shows the limiting behaviour, according to Laporte's calculations, as the contraction ratio tends to infinity. The transmitted shock is still of finite strength, and it is not difficult to see that this must be so. Laporte uses model 2(b) with the conditions behind the reflected shock equivalent to those for reflection from a solid wall. In particular, if p_* and a_* are the pressure and the speed of sound behind the reflected shock, then it follows that

$$\frac{p_*}{p_1} = \frac{p_2}{p_1}\,\frac{(3\gamma-1)p_2/p_1 - (\gamma-1)}{(\gamma-1)p_2/p_1 + (\gamma+1)}, \tag{2.8}$$

$$\frac{a_*^2}{a_1^2} = \frac{\{(3\gamma-1)p_2/p_1 + (\gamma-1)\}\{(\gamma-1)p_2/p_1 + 1\}}{\gamma\{(\gamma+1)p_2/p_1 + (\gamma-1)\}}. \tag{2.9}$$

The fluid velocity q_5, and speed of sound a_5 immediately upstream of the expansion are connected by

$$q_5^2 + \frac{2}{\gamma-1}a_5^2 = \frac{2}{\gamma-1}a_*^2, \tag{2.10}$$

and since $q_5 = a_5$ this implies that

$$q_5^2 = a_5^2 = \frac{2}{\gamma+1}a_*^2. \tag{2.11}$$

Also, across the expansion wave,

$$q_4 + \frac{2}{\gamma-1}a_4 = q_5 + \frac{2}{\gamma-1}a_5 = \frac{\gamma+1}{\gamma-1}\left(\frac{2}{\gamma+1}\right)^{1/2}a_*, \tag{2.12}$$

or, equivalently,

$$q_4 + \frac{2}{\gamma-1}a_4\left(\frac{p_4}{p_*}\right)^{\frac{\gamma-1}{2\gamma}} = \frac{\gamma+1}{\gamma-1}\left(\frac{2}{\gamma+1}\right)^{1/2}a_*. \tag{2.13}$$

Now the velocity and pressure are continuous across the contact discontinuity so that

$$\frac{q_3}{a_1} + \frac{2}{\gamma - 1}\frac{a_*}{a_1}\left\{\frac{p_3}{p_1}\cdot\frac{p_1}{p_*}\right\}^{\frac{\gamma-1}{2\gamma}} = \frac{\gamma+1}{\gamma-1}\left(\frac{2}{\gamma+1}\right)^{1/2}\frac{a_*}{a_1}. \tag{2.14}$$

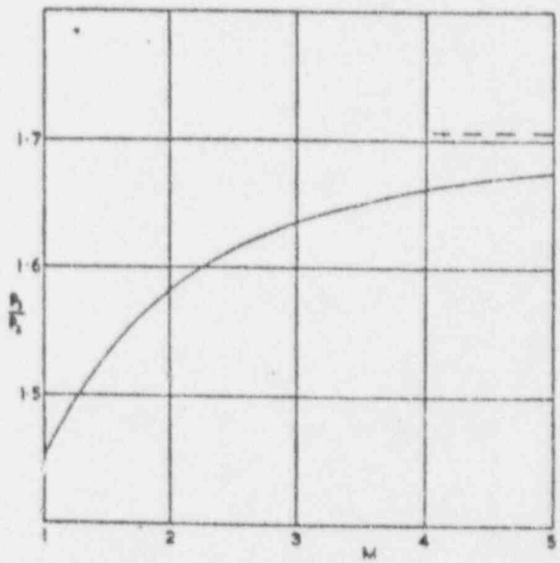

FIG. 5. The ratio of the pressures behind the transmitted and incident shocks as a function of the Mach number of the incident shock; steady state theory. $\gamma = 5/3$ and $\infty : 1$ contraction ratio.

In (2.14), q_3/a_1 can be obtained in terms of p_3/p_1 from the shock transition relations. It is in fact given by

$$\frac{q_3}{a_1} = \frac{1}{\gamma+1}\left(\frac{2}{\gamma}\right)^{1/2}\frac{(\gamma+1)p_3/p_1 - (\gamma-1)}{\{(\gamma+1)p_3/p_1 + (\gamma-1)\}^{1/2}} \tag{2.15}$$

Also p_*/p_1 and a^*/a_1 are expressible in terms of p_2/p_1 by (2.8) and (2.9) respectively. It follows that (2.14) can be used to determine p_3/p_1 as a function of p_2/p_1. Fig. 4(c) shows the result of such a calculation.

A further interesting property of this limiting solution for infinite contraction ratio is that a shock of substantial strength is transmitted, according to this model, even when the incident shock is weak. For in the limit of a weak incident shock $a_* \to a_1$, $p_* \to p_1$ and so equation (2.14) gives

$$\frac{1}{\gamma+1}\left(\frac{2}{\gamma}\right)^{1/2}\frac{(\gamma+1)p_3/p_1-(\gamma-1)}{\{(\gamma+1)p_3/p_1+(\gamma-1)\}^{1/2}}+\frac{2}{\gamma-1}\left(\frac{p_3}{p_1}\right)^{\frac{\gamma-1}{2\gamma}} = \frac{\gamma-1}{\gamma-1}\left(\frac{2}{\gamma-1}\right)^{1/2} \tag{2.16}$$

When $\gamma = 5/3$, (2.16) gives $p_3/p_1 = 1.453$. This feature of the solution is not brought out in Fig. 4 and accordingly p_3/p_2 is shown in Fig. 5 as a function of the Mach number of the incident shock.

A comparison of the three curves in Fig. 4 shows that the ratio of the pressure differences across the transmitted and incident shocks initially decreases with increasing shock strength, and reaches a minimum at roughly $M = 5$ for the 2 : 1 contraction and $M = 4$ for the 5 : 1 and ∞ : 1 contraction. After the minimum the ratio rises to its asymptotic value shown by the horizontal broken line in the figures. This increase is quite small. In fact for $M > 3$ the ratio changes by only 0.4% of itself for the ∞ : 1 contraction, and the change is even smaller in the other two cases.

The strength of the transmitted shock is very sensitive to the contraction ratio for weak shocks. There is, however, a marked decrease in sensitivity when the shock is strong. This can be seen from Table 1, where the values of $(p_3 - p_1)/(p_2 - p_1)$ are shown, for various contraction ratios, in the limit as $M \to \infty$.

TABLE 1 THE LIMITING VALUES, AS $M \to \infty$, OF THE RATIO OF THE PRESSURE DIFFERENCES ACROSS THE TRANSMITTED AND INCIDENT SHOCKS. STEADY STATE THEORY

Contraction Ratio	$(p_3 - p_1)/(p_2 - p_1)$	
	$\gamma = 5/3$	$\gamma = 7/5$
2 : 1	1.260	1.246
5 : 1	1.492	1.374
∞ : 1	1.706	1.511

Laporte's detailed calculations also show that there is a transition from model 2(a) to model 2(b) when M is about 2.4 for the 2 : 1 contraction, and 2.1 for the 5 : 1 contraction (Laporte's calculations are all based on these two models).

Finally it appears that the contact discontinuity between regions 3 and 4 is insignificant except for very strong shocks. In the range $2 < M < 7$ the density ratio (ρ_4/ρ_3) across this discontinuity varies between 1.03 and 1.0[illegible]

of the transmitted shock has a minimum, and there is another turning point at $M = 1.18$. The calculations were not sufficiently detailed to make reliable predictions, but it is possible that the turning point at $M = 1.18$ is associated with the onset of sonic conditions in region 5, and that at $M = 1.5$ with the entry of the stationary shock into the downstream section. There is, however, no conclusive evidence that they are in fact connected with the transition between the models of Fig. 3.

The results agree well with Parks's experiments using a 1 : 4 expansion and incident shock strengths within the range $3 < M < 5$ [19]. Note that $(p_3 - p_1)/(p_2 - p_1)$ approaches its asymptotic value for large M much more slowly than for a contraction.

Fig. 7 shows the limiting value of $(p_3 - p_1)A_1/(p_2 - p_1)A_2$ as $A_1/A_2 \to \infty$. It was assumed in the calculations that the stationary shock in the transition section never moved into the downstream section, so that the downstream flow was everywhere subsonic.

Note that Figs. 6 and 7 show the same qualitative behaviour for weak shocks.

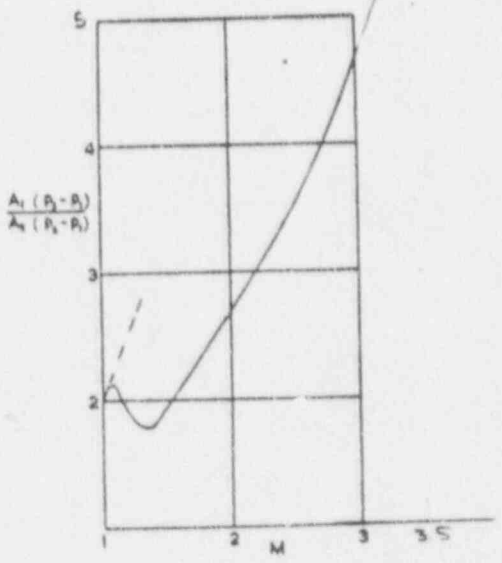

FIG. 7. The limiting value, as $A_1/A_2 \to \infty$, of $(p_3 - p_1)A_1/(p_2 - p_1)A_2$: steady state theory. $\gamma = 7/5$ and 1 : ∞ expansion ratio.

III. Chisnell's Theory

1. *Introduction*

The approach used in this section is quite different from the steady state theory described in Section II. Although the results of the latter theory are in fact verified when the area change is small (see for example [5]), in its generality Chisnell's theory deals more appropriately with the continuously changing shock strength as a function of that cross-sectional area of the duct occupied by the shock at any particular instant.

The problem is first considered for a small change in cross-sectional area. Chisnell's extension to arbitrary area changes is then explained and criticized. Two estimates of the accuracy of the result, by Chisnell [5] and by Whitham [7], are discussed and a comparison is made with a known